Available online at www.sciencedirect.com
ScienceDirect
Earth and Planetary Science Letters 261 (2007) 649–661
EPSL
www.elsevier.com/locate/epsl

Re–Os depositional ages and seawater Os estimates for the Frasnian–Famennian boundary: Implications for weathering rates, land plant evolution, and extinction mechanisms

Steven C. Turgeon [a,*], Robert A. Creaser [a], Thomas J. Algeo [b]

[a] Department of Earth and Atmospheric Sciences, University of Alberta, Edmonton, Alberta, Canada T6G 2E3
[b] Department of Geology, University of Cincinnati, Cincinnati, Ohio 45221-0013, USA

Received 5 June 2007; received in revised form 14 July 2007; accepted 19 July 2007
Available online 24 July 2007
Editor: H. Elderfield

Abstract

Four TOC-rich shale intervals spanning the Frasnian–Famennian (F–F) boundary were recovered in a drillcore (West Valley NX-1) from western New York (USA) and radiometrically dated using Re–Os. Two of the black shale intervals (WVC785 from ~2.9 m below, and WVC754 from ~6.4 m above the F–F boundary, respectively) yielded statistically overlapping ages with uncertainties of <1.1%. An interpolated age and associated graphically determined uncertainty of 372.4±3.8 Ma provides new absolute age constraints on the F–F boundary. This date is ~4.1 Ma younger than the latest proposed F–F boundary age of 376.1 Ma obtained by interpolation of U–Pb dates from volcanic zircon [Kaufmann, B., 2006. Calibrating the Devonian Time Scale: A synthesis of U–Pb ID-TIMS ages and conodont stratigraphy. Earth-Science Reviews 76, 175–190], and within uncertainty of the International Commission on Stratigraphy accepted date of 374.5±2.6 Ma. A third date (from sample WVC802, ~8.2 m beneath the F–F boundary) yielded an imprecise age of 357±23 Ma, owing in part to a limited Re/Os range. The initial $^{187}Os/^{188}Os$ (0.45 to 0.47), reflecting contemporaneous seawater Os values, are low but similar to the value of 0.42 reported for the Exshaw Fm (Canada) at the Devonian–Mississippian boundary (ca. 361 Ma) [Selby D., Creaser R.A., 2005. Direct radiometric dating of the Devonian–Mississippian time-scale boundary using the Re–Os black shale geochronometer. Geology 33, 545–548]. This may suggest fairly constant and low global continental weathering rates during the Late Devonian, although in view of the short residence time of Os in seawater ($\sim 1–4 \times 10^4$ yr), further measurements are needed to assess potential short-term variation in seawater Os ratios. Owing to low Os and Re abundances at the F–F boundary, our data are inconsistent with long-term volcanism and bolide impact as potential Late Devonian mass extinction mechanisms. In addition, the Frasnian–Famennian ocean appears to have been depleted with respect to Re, possibly indicating an exhaustion of the Re seawater reservoir owing to high burial rates of redox-sensitive elements under dysoxic/anoxic conditions leading up to the F–F boundary.

Keywords: Re–Os; geochronology; Frasnian–Famennian; Late Devonian mass extinction; black shales

1. Introduction

The Frasnian–Famennian (F–F) boundary marked the culmination of the prolonged (up to 3×10^6 yr;

* Corresponding author.
E-mail address: turgeonsc@ualberta.ca (S.C. Turgeon).

0012-821X/$ - see front matter © 2007 Elsevier B.V. All rights reserved.
doi:10.1016/j.epsl.2007.07.031

McGhee, 1996) Late Devonian mass extinction, one of the five greatest biotic crises of the Phanerozoic. During this event, up to 82% of marine species became extinct (Jablonski, 1991), with severe and highly selective decimation of low-latitude and shallow-water species of organisms such as reef-building corals and stromatoporoids (Copper, 1986; Stearn, 1987) and brachiopods (McGhee, 1996). Several hypotheses relating to extinction onset have been proposed, including bolide impact (McLaren, 1970), sea-level variations (Johnson, 1974), global warming (Thompson and Newton, 1988), global ocean anoxia (e.g., Joachimski and Buggisch, 1993), as well as multi-mechanism scenarios involving biogeochemical feedback (Buggisch, 1991; Sageman et al., 2003).

In addition to the marine realm, terrestrial ecosystems were subjected to major changes, mainly through the appearance of trees with large, extractive root systems (Chaloner and Sheerin, 1979; Mosbrugger, 1990; Meyer-Berthaud et al., 1999) and the appearance of seed plants capable of colonising largely barren drier upland habitats (representing ~90% of continents; Scheckler, 2003), in the mid- to late Famennian (Scheckler, 1986; Marshall and Hemsley, 2003). As a result, soils underwent deepening, horizonation, and compositional maturation (Retallack, 1997).

This rhizosphere development had important consequences for weathering rates and processes: prior to the soil and regolith stabilisation effect of a fully developed vegetative cover, weathering rates may have increased, at least ephemerally, owing to the upland colonisation (Algeo et al., 2001). Evidence of such an increase in weathering rates includes sediment-mass anomalies and clay mineral assemblages (Algeo et al., 1995), seawater $^{87}Sr/^{86}Sr$ values (Denison et al., 1997), and paleomagnetic susceptibility data (Crick et al., 2002; Hladil, 2002).

Furthermore, an increase in weathering could have enhanced the nutrient supply to the ocean realm, thereby enhancing primary productivity during this time interval (Algeo et al., 1995). This would have contributed to the development of pervasive anoxia on epicontinental seaways leading to the sequestration of large quantities of organic matter and authigenic pyrite in organic-rich ("black") shales (Ettensohn et al., 1988; Klemme and Ulmishek, 1991).

Several studies have applied the Re–Os isotope system to the geochronology of black shales (Ravizza and Turekian, 1989; Cohen et al., 1999; Singh et al., 1999; Creaser, 2002; Creaser et al., 2002; Selby and Creaser, 2003, 2005), including sediments subjected to chlorite-grade metamorphism (Kendall et al., 2004). Owing to redox reactions at or below the sediment–water interface, the organic matter of anoxic sediments is typically enriched in seawater-derived (hydrogenous) Re and Os (Ravizza and Turekian, 1989, 1992; Ravizza

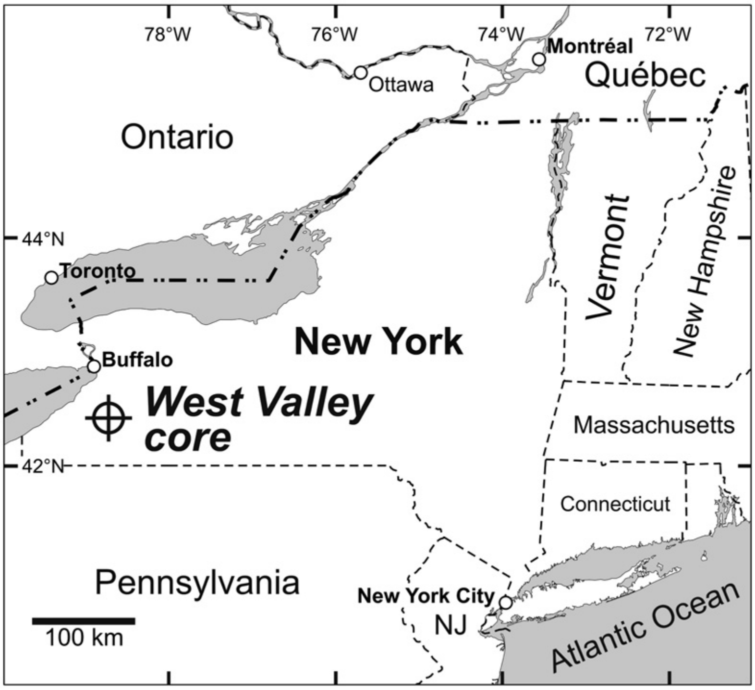

Fig. 1. Location of the West Valley NX-1 core.

et al., 1991; Martin et al., 2000; Creaser et al., 2002; Selby and Creaser, 2003). After deposition, ^{187}Re decays (β^-) to ^{187}Os over long time periods ($t_{1/2}$>41.6 Ga; Smoliar et al., 1996; Selby et al., 2007), and accumulates in the sediments, and can thus be a useful geochronometer assuming that the Re–Os system remains closed and that negligible non-hydrogenous Re and Os components are present (Ravizza and Turekian, 1989, 1992; Ravizza et al., 1991; Cohen et al., 1999; Creaser, 2002; Creaser et al., 2002; Selby and Creaser, 2003).

In this study, we present rhenium and osmium isotopic data for four TOC-rich black shale intervals spanning the F–F boundary within the Hanover Formation in the Appalachian basin of western New York. The aim of this research is to provide a chronological marker for the F–F boundary through Re–Os ages, as well as to constrain Late Devonian seawater Os isotopic composition, which should be reflective of the relative balance between Os inputs provided by global weathering and the volcanic/extraterrestrial contribution during the Late Devonian (Ravizza and Esser, 1993; Singh et al., 1999; Cohen, 2004). As well, the implications of our data regarding trigger mechanisms for the Late Devonian mass extinction will be discussed.

2. Samples and stratigraphic setting

Samples were collected from the West Valley NX-1 core, drilled in Cattaraugus County, western NY, USA (Fig. 1). This location was situated on the distal part of the northern Appalachian foreland basin during the Late Devonian (Sageman et al., 2003). Rhenium–osmium isotopic data were determined for four organic-rich shale intervals (~0.4–4% TOC; thickness ~30 cm each) spanning the F–F boundary (Fig. 2). These black shales are typically laminated, with minor bioturbated intervals and disseminated silt lenses, and are characterised by low thermal maturity indices (%R_o ~0.5 and CIA<2; Weary et al., 2000). The area's geology has been described in detail elsewhere (e.g. Sageman et al., 2003).

Three of our four samples are located within the upper part of Zone 13 of Klapper's (1997) Frasnian conodont zonation, most probably within the *linguiformis* conodont biozone (Over, 1997) of the upper Hanover Formation: sample WVC777 is situated below (ca. 80 cm) the F–F boundary, and is constrained within the Upper Kellwasser Event of Europe (Murphy et al., 2000), while samples WVC802 and WVC785 are located ~8.2 m and ~2.9 m beneath the F–F boundary, respectively. The Frasnian stage is approximately 300 m thick in the study area (Sageman et al., 2003). In addition to the extinction

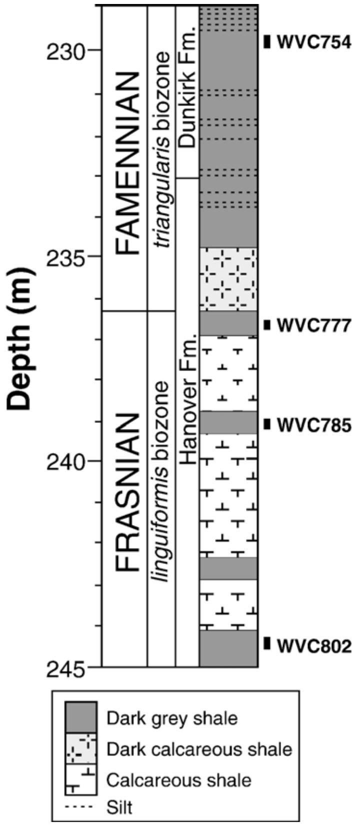

Fig. 2. Lithology and location of the WVC samples. Conodont biozones follow Kirchgasser et al. (1994), Klapper and Becker (1999), and Over (1997, 2002).

of all *Ancyrodella* and *Ozarkodina* conodonts and the loss of most species of *Palmatolepis*, *Polygnathus* and *Ancyrognathus*, the base of the Famennian is defined as the first occurrence of *Palmatolepsis triangularis* (Klapper et al., 1993). Sample WVC754 is located ~6.4 m above the F–F boundary, in the Middle *triangularis* conodont biozone of the Dunkirk Formation (Over, 1997). A lithologic description of the NX-1 core, as well as several organic and inorganic geochemical parameters, can be found in Sageman et al. (2003) and references therein.

3. Methodology

Large (>30 g) sub-samples were selected from each black shale interval in order to minimise potential small-scale disturbance of the Re–Os system (Kendall et al., 2004); these were powdered using non-metallic methods in order to avoid potential contamination by Os- or Re-bearing metallic particles (Creaser et al., 2002). All analyses were performed at the Radiogenic Isotope Facility of the Department of Earth and Atmospheric

Table 1
Re and Os data for the WVC black shale samples in this study

Sample[a]	Re (ng/g)	Os (pg/g)	$^{187}Re/^{188}Os$ [b]	$^{187}Os/^{188}Os$ [b]	[c]
WVC754-18	22.63	311.8	506.26±2.26	3.5599±0.0168	0.567
WVC754-18R	23.07	316.3	508.11±2.31	3.5448±0.0203	0.503
WVC754-17	24.56	300.5	598.90±2.65	4.1192±0.0126	0.441
WVC754-17R	25.84	316.2	598.34±5.87	4.1126±0.0203	0.224
WVC754-15	11.62	225.3	323.55±1.62	2.4395±0.0101	0.466
WVC754-15R	11.13	234.8	290.37±1.35	2.2084±0.0106	0.549
WVC754-14	11.88	216.5	349.93±1.72	2.6023±0.0100	0.479
WVC754-14R	12.04	235.6	317.93±1.34	2.3577±0.0111	0.508
WVC754-14R	11.87	216.0	350.38±1.64	2.6051±0.0123	0.586
WVC754-[11-12]	0.7311	50.03	78.924±1.90	1.0528±0.0106	0.345
WVC754-10	11.29	212.4	335.57±1.78	2.5022±0.0153	0.579
WVC754-10R	11.52	205.4	358.43±1.85	2.6311±0.0165	0.583
WVC754-9	19.36	258.6	528.49±2.54	3.6897±0.0150	0.471
WVC754-9R	18.81	258.5	506.99±2.55	3.5460±0.0227	0.533
WVC754-8	24.62	314.4	565.02±2.60	3.9387±0.0213	0.541
WVC754-8R	25.00	330.5	535.06±2.21	3.7126±0.0168	0.510
WVC754-7	18.58	237.1	565.09±2.95	3.9304±0.0239	0.600
WVC754-7R	18.90	239.9	568.24±3.36	3.9376±0.0360	0.509
WVC754-7R	18.88	241.6	564.82±2.75	3.9583±0.0235	0.558
WVC754-[2-5]	4.738	91.28	326.10±2.64	2.4569±0.0177	0.658
WVC754-[2-5]R	4.406	84.97	327.25±2.68	2.5024±0.0174	0.709
WVC777-11	4.002	161.8	137.92±1.04	1.3341±0.0123	0.374
WVC777-11R	4.002	162.1	137.83±1.20	1.3441±0.0168	0.411
WVC777-9	4.193	168.3	139.06±0.88	1.3392±0.0056	0.413
WVC777-5	3.642	153.4	132.03±0.93	1.3054±0.0065	0.426
WVC777-4	3.526	154.4	126.30±0.90	1.2600±0.0074	0.366
WVC777-3	3.420	155.5	120.69±0.88	1.1923±0.0071	0.394
WVC777-3R	3.420	155.5	120.73±0.91	1.1952±0.0085	0.382
WVC777-1	3.287	135.3	135.53±0.98	1.3346±0.0059	0.441
WVC785-14	9.029	109.5	614.22±4.45	4.3136±0.0292	0.739
WVC785-13	14.40	163.0	682.06±3.79	4.7444±0.0220	0.643
WVC785-9A	12.53	183.5	469.88±2.45	3.4105±0.0146	0.549
WVC785-9	9.219	134.6	472.44±3.06	3.4336±0.0228	0.600
WVC785-9R	9.445	129.4	503.81±4.16	3.4440±0.0374	0.579
WVC785-8	13.41	179.2	534.21±2.87	3.8199±0.0169	0.596
WVC785-8R	13.27	188.3	489.28±2.98	3.5033±0.0245	0.528
WVC785-5	14.52	186.9	562.87±3.04	3.9842±0.0192	0.568
WVC785-5R	14.90	53.05	537.75±6.03	3.8465±0.0681	0.561
WVC785-4	12.45	163.7	545.65±2.97	3.8790±0.0173	0.609
WVC785-3	21.80	224.8	789.28±3.98	5.4081±0.0221	0.564
WVC785-3R	21.58	224.4	776.36±4.78	5.3081±0.0373	0.557
WVC785-3R	21.58	226.3	764.36±3.99	5.2126±0.0257	0.522
WVC802-18	31.03	376.9	601.50±2.61	4.0862±0.0128	0.394
WVC802-17	30.52	371.6	598.43±2.66	4.0548±0.0147	0.387
WVC802-15	40.86	446.4	702.34±3.35	4.6704±0.0225	0.414
WVC802-14	39.39	441.8	677.48±2.84	4.5506±0.0133	0.356
WVC802-14R	38.23	426.9	679.65±3.18	4.5362±0.0109	0.320
WVC802-12	39.91	472.1	620.86±2.70	4.1461±0.0151	0.365
WVC802-12R	39.11	435.5	682.16±3.26	4.5451±0.0141	0.318
WVC802-8	34.12	409.8	612.23±2.64	4.1595±0.0147	0.352
WVC802-5	31.14	373.1	613.75±2.69	4.1591±0.0147	0.373
WVC802-4	31.32	372.7	618.46±3.05	4.1702±0.0167	0.310
WVC802-3	25.49	336.0	535.17±2.66	3.6840±0.0187	0.457
WVC802-3R	25.44	337.0	531.32±2.25	3.6594±0.0096	0.394

Sciences, University of Alberta, using 0.5 g of powdered sediment and following the $Cr^{VI}O_3$–H_2SO_4 digestion procedure of previous studies (Selby and Creaser, 2003; Kendall et al., 2004).

Purified analytes were loaded onto Ni (for Re) and Pt (for Os) filaments, and concentration and isotopic compositions measured using isotope dilution on a VG Sector 54 thermal ionization mass spectrometer in negative ion mode (Creaser et al., 1991; Völkening et al., 1991). Rhenium analyses were performed on Faraday collectors in static mode, while osmium samples were analysed using a single pulse counter in peak jumping-mode. Isotopic ratios were corrected for instrumental mass fractionation using ^{185}Re/^{187}Re = 0.59738 (Gramlich et al., 1973) and ^{192}Os/^{188}Os = 3.08261 (Nier, 1937), isobaric oxygen interferences, spike and blank contributions. Total procedural blanks were < 15 and < 0.5 pg for Re and Os, respectively, with ^{187}Os/^{188}Os values of ~ 0.20. In-house standard solutions were repeatedly analysed to monitor long-term mass spectrometer reproducibility. Errors for isotope ratios were determined by numerical error propagation and include uncertainties in spike calibration, weighing, and analytical/instrumental measurements, as well as Re bias, oxygen, and blank corrections.

All dates (quoted at the 2σ level) were determined through the regression of the Re–Os data using the Isoplot 3 program (Ludwig, 2003), and a ^{187}Re decay constant (λ^{187}Re) of 1.666×10^{-11} yr^{-1} (±0.35%) (Smoliar et al., 1996); calculated uncertainties for the ^{187}Re/^{188}Os values, the 2σ_m (which includes blank corrections) for the ^{187}Os/^{188}Os ratios, and the error correlation (ρ or rho; Ludwig, 1980) between ^{187}Re/^{188}Os and ^{187}Os/^{188}Os, which ranges from ~ 0.3 to 0.7, were used for regression analysis.

4. Results

The samples contain between 0.7–41 ng/g Re and 50–472 pg/g Os, with ^{187}Re/^{188}Os and ^{187}Os/^{188}Os ratios ranging from ~ 79 to 789, and from ~ 1.2 to 5.4, respectively (Table 1). Regression of the Re–Os data for the WVC785 (n = 8) and WVC754 (n = 9) intervals yield Model 1 isochrons of 374.2 ± 4.0 Ma (1.1% 2σ age uncertainty; mean square weighted deviates, or MSWD = 0.51; probability of fit = 0.80) and 367.7 ± 2.5 Ma (0.68% 2σ age uncertainty; MSWD = 1.4; probability of fit = 0.21) respectively (Fig. 3A and C). Initial ^{187}Os/^{188}Os values, which have been derived from these regressions, are 0.47 ± 0.04 and 0.45 ± 0.02 for WVC785 and 754, respectively.

In order to provide a more robust comparison with other published dates, the above isochron dates (WVC785 and WVC754) have been adjusted for the ^{187}Re decay constant uncertainty. λ^{187}Re has been verified using our standard solution and comparing Re–Os ages from molybdenites against U–Pb dates from zircons from magmatic ore systems (Selby et al., 2007). This study has obtained an average λ^{187}Re value of 1.66785×10^{-11} yr^{-1} (± ~ 0.20% at 2σ), which is almost identical to the decay constant of Smoliar et al. (1996). By propagating the regression slope uncertainty (determined by Isoplot) in addition with a 0.35% uncertainty for λ^{187}Re, the decay constant adjusted uncertainties for WVC785 and WVC754 are 374.2 ± 4.2 Ma and 367.7 ± 2.8 Ma respectively (at 2σ).

Whereas the previous two sample intervals yielded Model 1 isochrons, samples from the WVC777 interval (n = 6), with their limited spread in isotopic data (^{187}Os/^{188}Os = ~ 1.18 to 1.35 and ^{187}Re/^{188}Os = 120 to 140), yield a Model 3 isochron with a high 2σ age uncertainty (470 ± 140 Ma; MSWD = 11.7; initial ^{187}Os/^{188}Os = 0.24 ± 0.31; Fig. 3B), and hence cannot be used as a reliable geochronometric anchor. In addition to the restricted isotopic range, the Re and Os contents of the WVC777 samples are the lowest of the four studied intervals (3.68 ng/g and 155 pg/g, respectively, on average; Table 1).

The isochron for the WVC802 interval samples shows six (out of nine) data points plotting in a tight cluster around ^{187}Os/^{188}Os = 4.1 and ^{187}Re/^{188}Os ~ 610 (Fig. 3D). In large part owing to this center-weighted distribution, the Model 3 isochron generated by Isoplot is imprecise (357 ± 23 Ma; MSWD = 5.9; initial ^{187}Os/^{188}Os = 0.49 ± 0.24) and thus cannot be used as a reliable indicator of depositional age.

5. Discussion

5.1. Frasnian–Famennian boundary age

Fig. 4 shows our two Model 1 Re–Os dates (WVC754 and WVC785) plotted along four previously

Notes to Table 1:
[a]Samples marked “R” indicate replicate analyses. Note that sample WVC754-[11-12] (grey shading) was not included for isochron determination owing to anomalously low Re content. [b]Uncertainties calculated by numerical error propagation and quoted as 2σ. [c]ρ (or rho) is the associated error correlation (Ludwig, 1980).

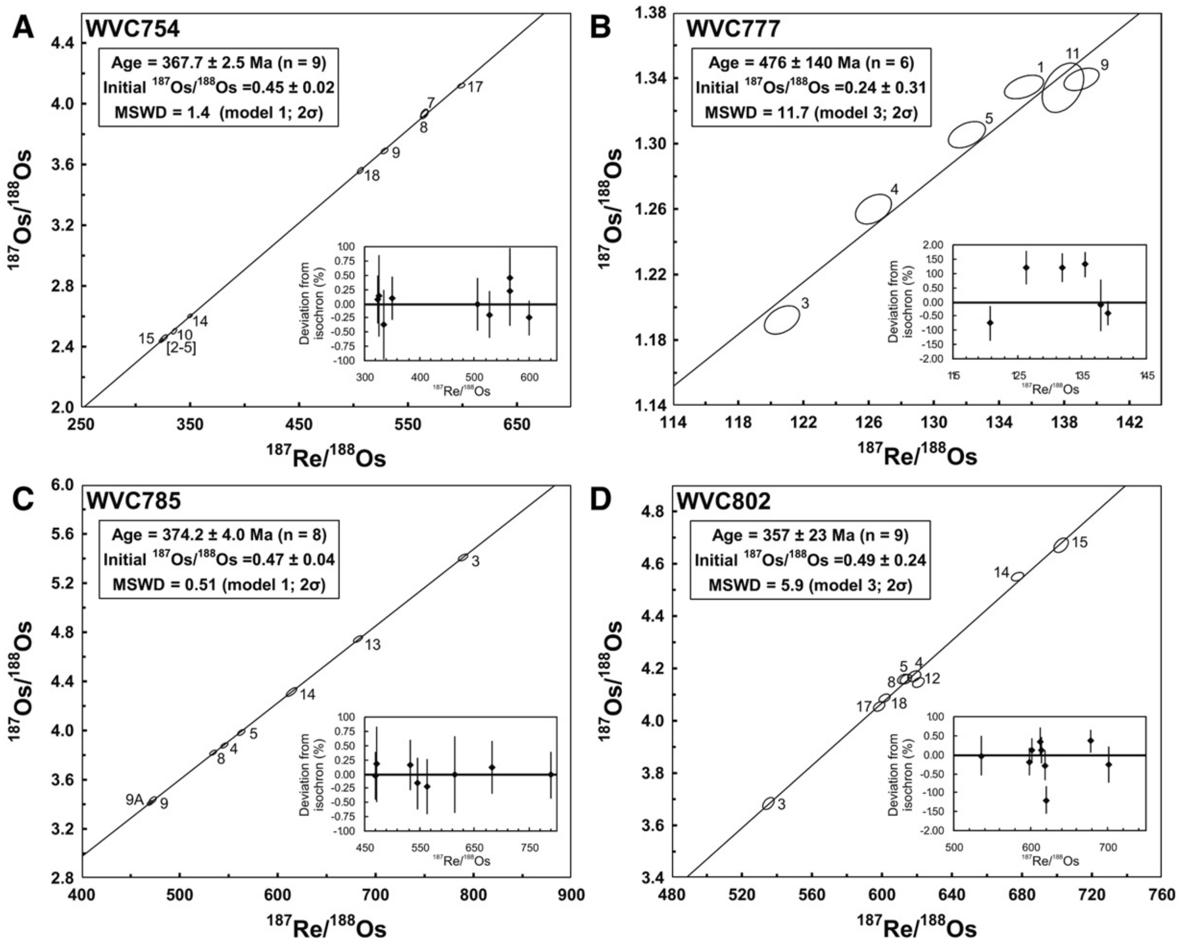

Fig. 3. Isochrons for the four studied black shale intervals close to the Frasnian–Famennian boundary in the West Valley NX-1 core: A) WVC754; B) WVC777; C) WVC785, and; D) WVC802. Ellipses are propagated 2σ uncertainties and sample numbers are linked with data in Table 1. Replicate analyses are not included. The inset diagrams show the deviation of data points relative to isochron regression lines. The dates do not include the λ^{187}Re-related uncertainty.

published, non-decay constant uncertainty adjusted, biostratigraphically constrained (to either the Frasnian or Famennian stages) U–Pb ID-TIMS dates:

1. Tucker et al. (1998) report nine single-grain and small-fraction (up to $n=25$) zircon analyses from the lowermost ash bed the Belpre ash suite of the Chattanooga Shale at Little War Gap, Tennessee (Rotondo and Over, 2000), which yielded two concordant and seven discordant analyses, but with a common ^{207}Pb/^{206}Pb age of 381.1 ± 1.3 Ma. The conodont *Palmatolepis punctata* is found in the interval surrounding the ash layer, whereas shales between the two youngest Belpre ash beds contain the conodont *Ancyrognathus barba* (Rotondo and Over, 2000), effectively restricting the biostratigraphic age to the Frasnian Zone 8 (middle to upper part of the Lower *hassi* Zone; Ziegler and Sandberg, 1990; Klapper, 1997; Klapper and Becker, 1999).
2. Twenty-four single-grain analyses were performed on zircons extracted from a bentonite layer located between the two Kellwasser horizons (Kaufmann et al., 2004) in the middle part of the Upper *rhenana* conodont zone (Schindler, 1990; Ziegler and Sandberg, 1990) at Steinbruch Schmidt (Kellerwald, Germany). Seventeen concordant results yielded a cluster of ages scattered from 359.2 to 377.2 Ma owing to varying amounts of Pb loss. The oldest concordant ^{206}Pb/^{238}U age of 377.2 ± 1.7 Ma is thought to have the lowest amount of Pb loss, and is therefore assumed to represent the age of the bentonite-related eruption (Kaufmann et al., 2004).
3. The age of a miospore-bearing horizon of the Upper Devonian Carrow Formation of the Piskahegan

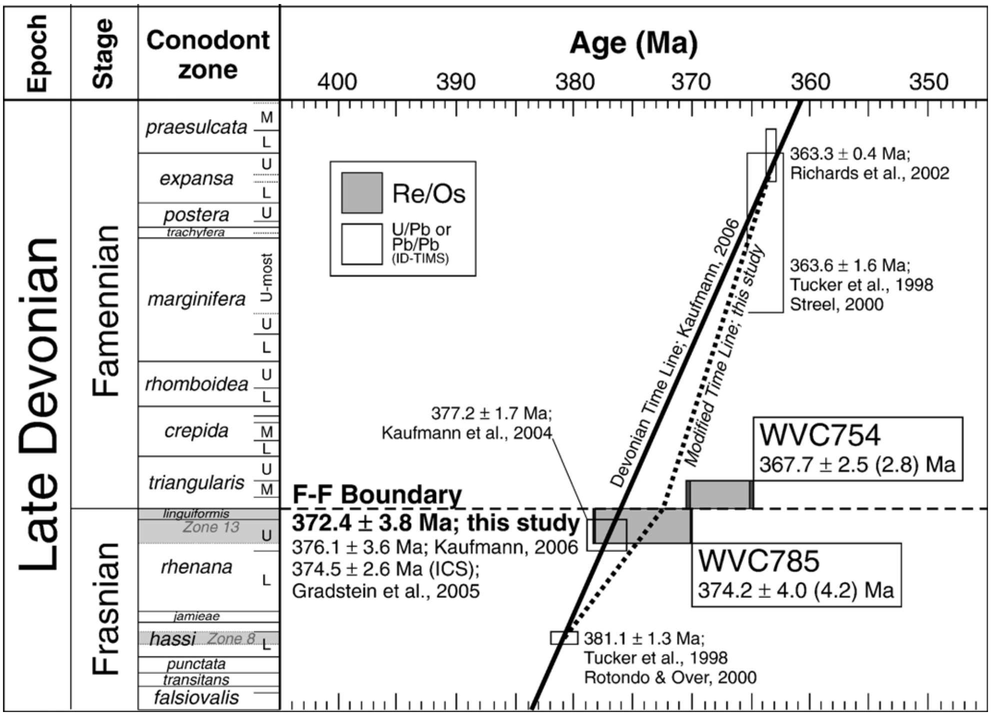

Fig. 4. Time-scale for the Frasnian–Famennian interval. Biozone divisions are based on the compilation of Kaufmann (2006) and references therein. Each U–Pb ID-TIMS data point discussed in the text is represented by a rectangle formed by 2σ age uncertainty interval and biostratigraphic range. The dark areas and numbers in parentheses for the Re–Os dates represent λ^{187}Re-inclusive uncertainties. Modified from Kaufmann, 2006.

Group (New Brunswick, Canada) is constrained by concordant $^{207}Pb/^{206}Pb$ analyses on zircons from an underlying pumiceous tuff member and an overlying rhyolite belonging to the Mount Pleasant Caldera Complex (McCutcheon et al., 1997). Four analyses (1–15 grains each) from the tuff yielded a weighed mean age of 363.8±2.2 Ma, whereas five multi-grain (n=2 to 25) analyses of the overlying Bailey Rock Rhyolite have a weighted mean age of 363.4±1.8 Ma (Tucker et al., 1998). Given that the ages of the two volcanic units are analytically indistinguishable, we quote Tucker et al.'s (1998) reported mean of all $^{207}Pb/^{206}Pb$ ages (363.6±1.6 Ma). Owing to a doubtful index fossil specimen (*Retizonomonoletes lepidophyta*?), the horizon was originally assumed to belong to the *pusillites–lepidophyta* miospore zone (equivalent to being located within the Upper *expansa* conodont zone; Ziegler and Sandberg, 1990) of the upper Famennian (McGregor and McCutcheon, 1988), but has more recently been attributed to *R. cassicula* (now *R. macroreticulata*) by Steemans et al. (1996). As *R. macroreticulata* appears in the Uppermost *marginifera* conodont zone in Belgium (Streel and Loboziak, 1996), the biostratigraphic range of the two dated volcanic rocks is now interpreted to range from the Uppermost *marginifera* to the Upper *expansa* conodont zone (Streel, 2000).

4. Four multi-grain analyses of monazites extracted from the Nordegg Tuff in the Exshaw Formation (Alberta, Canada) yielded a highly precise weighted mean $^{207}Pb/^{235}U$ age of 363.3±0.4 Ma (Richards et al., 2002). Biostratigraphic constraints for this sample come from Middle *Palmatolepis expansa* to the Lower *Siphonodella praesulcata* conodont-bearing nodular limestone beds from below and above the Nordegg Tuff (Savoy et al., 1999).

In Fig. 4, time is plotted on the X-axis, while the Y-axis represents stratigraphic age as defined by conodont zonation (Ziegler and Sandberg, 1990) and Late Devonian biozones (Klapper, 1997). The duration of the biostratigraphic divisions is based on the compilation of Kaufmann (2006), which is largely based on the Frasnian Composite Standard of Klapper (1997) and the Famennian portion of the Lali section located in southern China (Ji and Ziegler, 1993). The horizontal uncertainty for each data point constrains the 2σ precision of the isotopic age, while the vertical range reflects its biostratigraphic range. A straight "Time Line" can then be fitted to connect each box and provide direct age reading at any point along the line. Following this construction, Kaufmann (2006) obtained an age for the F–F boundary of 376.1 ± 3.6 Ma, which is similar to the age of 376.5 Ma obtained by Tucker et al. (1998) using a comparable approach. Gradstein et al. (2004), however, obtained a slightly younger age of 374.5 ± 2.5 Ma through statistical spline fitting to selected radiometric dates.

While one of our isochron dates (WVC785) is intersected by the Time Line of Kaufmann (2006), the date from the WVC754 isochron appears to be markedly (ca. 8.1 Ma) offset, falling outside the range of most of the recently published F–F age estimates. However, even though the MSWD of the WVC754 date is higher (1.4) compared to the WVC785 date (0.51), we find no compelling reason to exclude this date. A potential implication of the offset of this data point is the presence of a condensed section in the interval between the two dates, although there are no reports of hiatuses in the literature and sedimentation rates appear to be high (Sageman et al., 2003). Alternatively, the pattern of non-linearity shown between the Frasnian and Famennian could imply faster evolutionary rates for Famennian stage conodonts.

Assuming a linear sedimentation rate in the WVC core, the interpolation of our two Model 1 Re–Os dates yield a slightly younger age for the F–F boundary of 372.4 ± 3.8 Ma (uncertainty obtained by graphic interpolation). This date is ~1.0 to 1.1% younger than those obtained by Tucker et al. (1998) and Kaufmann (2006), and ~0.6% younger than the International Commission on Stratigraphy-accepted age of Gradstein et al. (2004) for the F–F boundary. These differences are higher, but of similar magnitude, than the ~0.2% variation in nominal age values for the age of the Devonian–Mississippian boundary obtained by Selby and Creaser (2005) by comparing their direct Re–Os isochron age with the interpolated U–Pb age of Trapp et al. (2004).

Modifying Kaufmann's (2006) Time Line to account for our proposed date, the Steinbruch Schmidt uncertainty box would no longer be intersected (Fig. 4). Hence, an adjustment of the biostratigraphic scale becomes necessary, which, given our data, would possibly involve an expansion of the uppermost Frasnian biozones (*linguiformis* and/or Upper *rhenana*, or Zone 13 of Klapper (1997)).

5.2. Implications of Late Devonian seawater Os isotope estimates

The present-day osmium isotope ($^{187}Os/^{188}Os$) composition of seawater is ~1.06 (Levasseur et al., 1998; Woodhouse et al., 1999; Peucker-Ehrenbrink and Ravizza, 2000), and reflects mass balance between the main Os input sources to the oceans, namely the hydrothermal alteration of juvenile oceanic crust, continental weathering, as well as a generally minor extraterrestrial contribution from meteorites (Cohen et al., 1999). While the extraterrestrial and hydrothermal inputs have similar isotopic ratios (~0.127), crustal Os isotopes show a wide range of values, from 0.127 to approximately 1.9, depending on the age of the crust and lithology (Martin et al., 2001; Peucker-Ehrenbrink and Hannigan, 2000). And although the Os isotopic composition of present-day oceans appears to be more or less uniform, the relative contributions of these sources in the past have led to significant, at times abrupt, variations in seawater Os isotope ratios (Cohen, 2004).

The Os isotopic system in oceans is similar to Sr isotopes, which also reflect a balance between weathering and volcanic activity. However, given that Os has a much shorter residence time (~$1–4\times10^4$ yr v. ~3×10^6 yr for Sr), the Os isotopic composition of seawater responds much more rapidly to relative shifts of the different inputs (Oxburgh, 1998; Ravizza et al., 2001; Ravizza and Peucker-Ehrenbrink, 2003; Cohen, 2004). In contrast to Sr isotopes though, the Os isotopic record can be influenced by extraterrestrial contributions from chondritic or iron meteorites as they contain abundant Os (Cohen et al., 1999).

Given that most of the Os in TOC-rich marine shales is hydrogenous (Cohen et al., 1999), the initial $^{187}Os/^{188}Os$ ratios defined by black shale-derived isochrons are representative of contemporaneous seawater (Ravizza and Turekian, 1989; Cohen et al., 1999). Fig. 5 shows the

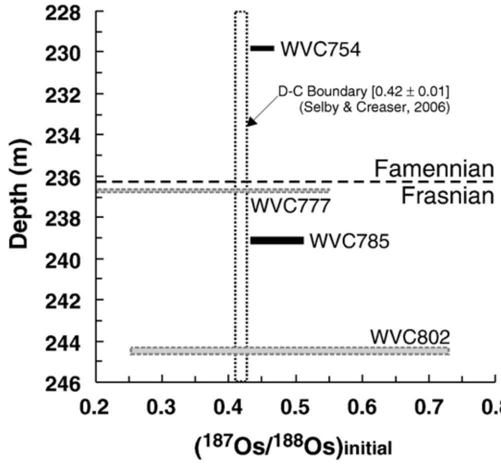

Fig. 5. Black bars represent osmium isotopes ratios for the two Model 1 isochrons (WVC785 and WVC754), while the grey bars are from the Model 3 isochrons (WVC802 and WVC777). The outlined vertical area shows the initial Os isotope range obtained by Selby and Creaser (2005) at the Devonian–Mississippian boundary.

initial $^{187}Os/^{188}Os$ ratios for the WVC samples across the F–F boundary. Our two Model 1 isochrons returned initial Os isotope values of 0.45±0.02 and 0.47±0.04 for WVC754 and WVC785 respectively. These values are similar to the initial ratio of 0.42±0.1 for the Devonian–Mississippian boundary reported by Selby and Creaser (2005).

While admittedly based on a limited dataset, two first-order implications of the Os record of late Frasnian and early Famennian seawater can be put forth: firstly, no significant trend can be observed in our data. Indeed, the isotopic values appear to remain more or less constant, possibly even shifting to slightly less radiogenic values, throughout the Late Devonian and up to the Mississippian. This suggests that the relative fluxes of the major Os inputs to oceans have remained somewhat steady, perhaps over time-scales of 10^6 yr, implying that any shift in upland colonisation by vegetation during this time had only a minor (slightly stabilising?) effect on weathering rates. Variations in weathering intensity could have still occurred during this time interval: for example, at times of minimal influx of extraterrestrial material and reduced volcanic activity, the weathering of crustal material with uniform Os isotopic composition similar to contemporaneous seawater could minimise or hide the impact of these changes in the Os record. As well, any weathering increase related to vegetation colonisation could have ended well before the Frasnian–Famennian transition and hence may not have been recorded in our sample set.

Secondly, in spite of the ambiguity of the initial Os isotope record directly at the F–F boundary, no clear evidence for bolide impact or volcanism exists for this interval. In contrast, the Os record at the K–T boundary (Pegram and Turekian, 1999) shows an abrupt excursion (<0.25 Myr) towards lower (~0.2) osmium isotope ratios, consistent with the widely held view of a bolide impact. As well, the lower Os content (155 pg/g) for this shale interval, relative to those sections above and below, excludes a significant Os influx from chondritic or iron meteorites, although the possibility remains for an impactor of a different nature (e.g. ice-cored).

The decreased Re and Os abundances in our WVC777 interval are also at odds with the high chemical weathering rates which have been reported for juvenile basaltic lavas (Louvat and Allègre, 1997; Taylor and Lasaga, 1999), which have been linked with long-term increases in Os and Re contents of sediments (Ravizza and Peucker-Ehrenbrink, 2003). The lack of significant volcanic activity at the F–F boundary is also documented by the $^{87}Sr/^{86}Sr$ ratio of seawater as it shows only a slight increase (from ca. 0.70780 to 0.70805, consistent with an increase in weathering or reduction in volcanic activity) over the entire Frasnian–Famennian interval (Denison et al., 1997).

5.3. Re and Os drawdown at the Frasnian–Famennian boundary?

Fig. 6 shows the relationships between Re, Os and TOC contents for the WVC samples. Fig. 6A illustrates the inverse relationship between average Os and Re contents and TOC for each interval. When plotting the individual samples within those intervals, however, positive correlations between Re and Os with TOC can be distinguished (Fig. 6B): these relationships are also reflected when plotting Re v. Os (Fig. 6C). The parallel nature of these trendlines within each black shale interval further indicates that Re and Os behave alike and that similar processes control their incorporation into black shales.

Two other features of the Fig. 6B trendlines should be noted: firstly, the slopes of these trendlines within each interval vary widely, with the steepest trendline slope found on the lowermost WVC802 interval, and shallowest slopes found within the WVC777 sample suite. The second feature is the offset between paired Re and Os trendlines within each black shale interval: the Re and Os trendlines for the WVC802 interval are virtually indistinguishable from each other (keeping in mind the difference in scale between the two elements — pg/g for Os and ng/g for Re), whereas the WVC777 interval shows a much increased relative offset between Re and Os.

Although speculative at this stage, we postulate that this relative decrease in Re (we assume here that Re contents have decreased, as Os contents in WVC777 are only marginally lower than WVC785 and WVC754, whereas Re decreases by ~3–9×) at the F–F boundary could represent a long-term drawdown in seawater Re contents, as hinted at by the trendlines in Fig. 6B. In this figure, the lowermost WVC802 interval has the highest Re and Os v. TOC ratios, followed by WVC785 and WVC777, which appears to indicate a generalized decrease towards the F–F boundary (WVC777); the ratios then increase from WVC777 to the WVC754 interval.

The increasing relative depletion of Re compared to Os, which parallels the decreasing Re and Os ratios, could be attributed to the efficient removal of Re from seawater under even slightly reducing conditions: the Frasnian–Famennian ocean thus appears to have been depleted with respect to Re, possibly indicating an exhaustion of the Re seawater reservoir owing to high

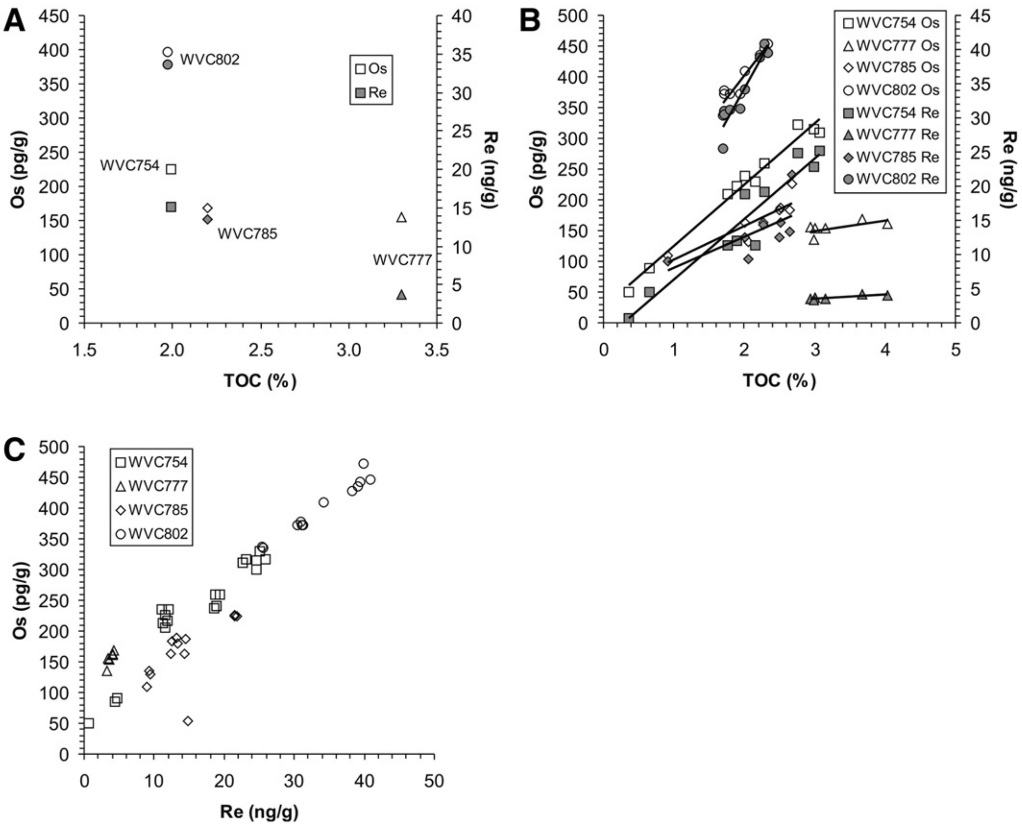

Fig. 6. Relationships between Re, Os and TOC contents: A) average Os and Re v. average TOC contents for the studied black shale intervals; B) Os and Re v. TOC contents for individual samples (thick black line are trendlines for each elements within a black shale interval), and C) Re–Os plot for individual samples.

burial rates of redox-sensitive elements under dysoxic/anoxic conditions (Algeo, 2004) leading up to the F–F boundary.

6. Conclusions

Re–Os isotope data were generated from four black shale intervals spanning the Frasnian–Famennian boundary from western New York (USA). Our proposed date for the F–F boundary of 372.4±3.8 Ma is slightly younger than the most recent calibration of Kaufmann (2006) of 376.1±3.6 Ma and of Gradstein et al. (2004) of 374.5±2.6 Ma, yet still remains within the uncertainty limits of these dates. This demonstrates that the Re–Os black shale geochronometer can be useful for refining the chronology of biostratigraphically defined boundaries, especially for time periods lacking material typically used for well-established U–Pb ID-TIMS and Ar–Ar dating procedures (i.e. zircons and other minerals from volcanic beds). As well, the precision of the Re–Os age determinations (±1.0%, including decay constant uncertainty) can help improve geologic time-scales, especially for intervals suffering from a paucity of absolute geochronologic anchors points, and aid in establishing the timing of events and rates of processes.

The initial $^{187}Os/^{188}Os$ (0.45 to 0.47), reflecting contemporaneous seawater Os values, are low, but similar to the value of 0.42 reported for the Exshaw Fm (Canada) at the Devonian–Mississippian boundary (361 Ma) (Selby and Creaser, 2005). These initial Os isotope values suggest constant and low global continental weathering rates during the Late Devonian, although the slightly decreasing trend could be in response to increased slope stabilisation effect brought on by upland colonisation by vegetation. In view of the short residence time of Os in seawater (~ 1–4×10^4 yr, which is less that $\sim 0.35\%$ of the duration of the Famennian stage), however, further measurements are needed to assess potential short-term variations in seawater Os ratios. In addition, initial Os determinations of earlier black shales (Frasnian or even older) could be useful to determine if this colonisation was complete at the F–F boundary, or if indeed vegetation had any effect on weathering rates. As well, our data appear to be inconsistent with long-term volcanism and/or bolide impact as potential Late Devonian mass extinction mechanisms owing to low Os and Re abundances at the F–F boundary.

Acknowledgements

Core material for this study was obtained from the New York State Geological Survey. This research was supported by a Natural Science and Engineering Research Council (NSERC) Discovery Grant to Creaser, and by the National Science Foundation grant EAR-0618003 to Algeo and Creaser. The Radiogenic Isotope Facility at the University of Alberta is supported in part by an NSERC Major Facilities Access Grant. Bernd Kaufmann and an anonymous reviewer provided constructive criticisms of this manuscript. We also thank Brian Kendall, Ryan Morelli for Re–Os-related discussions, as well as Jaime Hallowes, Gayle Hatchard, and Hilary Corlett for their technical assistance in sample preparation and analysis.

References

Algeo, T.J., 2004. Can marine anoxic events draw down the trace element inventory of seawater? Geology 32, 1057–1060.

Algeo, T.J., Berner, R.A., Maynard, J.B., Scheckler, S.E., 1995. Late Devonian Oceanic Anoxic Events and Biotic Crises: “Rooted” in the Evolution of Vascular Land Plants? Geol. Soc. Am. Today 5, pp. 45, 64–66.

Algeo, T.J., Scheckler, S.E., Maynard, J.B., 2001. Effects of the Middle to Late Devonian spread of vascular land plants on weathering regimes, marine biotas, and global climate. In: Gensel, P.G., Edwards, D. (Eds.), Plants Invade the Land: Evolutionary and Environmental Perspectives. Columbia University Press, New York, pp. 213–236.

Buggisch, W., 1991. The global Frasnian–Famennian “Kellwasser Event”. Geol. Rundsch. 80, 49–72.

Chaloner, W.G., Sheerin, A., 1979. Devonian macrofloras. In: House, M.R., Scrutton, C.T., Bassett, M.G. (Eds.), The Devonian system. Palaeontol. Soc. Spec. Pap., vol. 23, pp. 145–161.

Cohen, A.S., 2004. The rhenium–osmium isotope system: applications to geochronological and palaeoenvironmental problems. J. Geol. Soc. (Lond.) 161, 729–734.

Cohen, A.S., Coe, A.L., Bartlett, J.M., Hawkesworth, C.J., 1999. Precise Re–Os ages of organic-rich mudrocks and the Os isotope composition of Jurassic seawater. Earth Planet. Sci. Lett. 167, 159–173.

Copper, P., 1986. Frasnian–Famennian mass extinction and coldwater oceans. Geology 14, 835–839.

Creaser, R.A., 2002. A review of the rhenium–osmium (Re–Os) isotope system with application to organic-rich sedimentary rocks. In: Lentz, D.R. (Ed.), Geochemistry of Sediments and Sedimentary Rocks: Evolutionary Considerations to Mineral Deposit-Forming Environments. Geol. Assoc. Can. Geotext, vol. 4, pp. 63–67.

Creaser, R.A., Papanastassiou, D.A., Wasserburg, G.J., 1991. Negative thermal ion mass spectrometry of osmium, rhenium, and iridium. Geochim. Cosmochim. Acta 55, 397–401.

Creaser, R.A., Sannigrahi, P., Chacko, T., Selby, D., 2002. Further evaluation of the Re–Os geochronometer in organic-rich sedimentary rocks: a test of hydrocarbon maturation effects in the Exshaw Formation, Western Canada Sedimentary Basin. Geochim. Cosmochim. Acta 66, 3441–3452.

Crick, R.E., Ellwood, B.B., Feist, R., El Hassani, A., Schindler, E., Dreesen, R., Over, D.J., Girard, C., 2002. Magnetostratigraphy susceptibility of the Frasnian/Famennian boundary. Palaeogeogr. Palaeoclimatol. Palaeoecol. 181, 67–90.

Denison, R.E., Koepnick, R.B., Burke, W.H., Hetherington, E.A., Fletcher, A., 1997. Construction of the Silurian and Devonian seawater $^{87}Sr/^{86}Sr$ curve. Chem. Geol. 140, 109–121.

Ettensohn, F.R., Miller, M.L., Dillman, S.B., Elam, T.D., Geller, K.L., Swager, G., Markowitz, G.D., Woock, F.D., Barron, L.S., 1988. Characterization and implications of the Devonian–Mississippian black shale sequence, eastern and central Kentucky, U.S.A.: pycnoclines, transgression, and tectonism. In: McMillan, N.J., Embry, A.F., Glass, D.J. (Eds.), Devonian of the World, II. Can. Soc. Petrol. Geol. Mem., vol. 14, pp. 323–345.

Gradstein, F.M., Ogg, J.G., Smith, A.G., Agterberg, F.P., Bleeker, W., Cooper, R.A., Davydov, V., Gibbard, P., Hinnov, L.A., House, M.R., Lourens, L., Luterbacher, H.P., McArthur, J., Melchin, M.J., Robb, L.J., Shergold, J., Villeneuve, M., Wardlaw, B.R., Ali, J., Brinkhuis, H., Hilgen, F.J., Hooker, J., Howarth, R.J., Knoll, A.H., Laskar, J., Monechi, S., Plumb, K.A., Powell, J., Raffi, I., Röhl, U., Sadler, P., Sanfilippo, A., Schmitz, B., Shackleton, N.J., Shields, G.A., Strauss, H., Van Dam, J., van Kolfschoten, T., Veizer, J., Wilson, D., 2004. A Geologic Time Scale 2004. Cambridge University Press, Cambridge.

Gramlich, J.W., Murphy, T.J., Garner, E.L., Shields, W.R., 1973. Absolute isotopic abundance ratio and atomic weight of a reference sample of rhenium. J. Res. Natl. Bur. Stand. 77A, 691–698.

Hladil, J., 2002. Geophysical records of dispersed weathering products on the Frasnian carbonate platform and early Famennian ramps in Moravia, Czech Republic: proxies for eustasy and palaeoclimate. Palaeogeogr. Palaeoclimatol. Palaeoecol. 181, 213–250.

Jablonski, D., 1991. Extinctions: a paleontological perspective. Science 253, 754–757.

Ji, Q., Ziegler, W., 1993. Lali section: an excellent reference section for Upper Devonian in south China. CFS, Cour. Forsch.inst. Senckenb. 157, 183.

Joachimski, M.M., Buggisch, W., 1993. Anoxic events in the late Frasnian — causes of the Frasnian–Famennian faunal crisis? Geology 21, 675–678.

Johnson, J.G., 1974. Extinction of perched faunas. Geology 2, 479–482.

Kaufmann, B., 2006. Calibrating the Devonian Time Scale: A synthesis of U–Pb ID-TIMS ages and conodont stratigraphy. Earth-Sci. Rev. 76, 175–190.

Kaufmann, B., Trapp, E., Mezger, K., 2004. The numerical age of the Upper Frasnian (Upper Devonian) Kellwasser Horizons: a new U–Pb zircon date from Steinbruch Schmidt (Kellerwald, Germany). J. Geol. 112, 495–501.

Kendall, B.S., Creaser, R.A., Ross, G.M., Selby, D., 2004. Constraints on the timing of Marinoan “Snowball Earth” glaciation by ^{187}Re–^{187}Os dating of a Neoproterozoic, post-glacial black shale in Western Canada. Earth Planet. Sci. Lett. 222, 729–740.

Kirchgasser, W.T., Over, D.J., Woodrow, D.L., 1994. Frasnian (Upper Devonian) strata of the Genesee River Valley, western New York state. In: Brett, C.E., Scatterday, J. (Eds.), NY State Geol. Assoc., 66th Annual Meeting Field Trip Guidebook, pp. 325–358.

Klapper, G., 1997. Graphic correlation of Frasnian (Upper Devonian) sequences in Montagne Noire, France, and western Canada. In: Klapper, G., Murphy, M.A., Talent, J.A. (Eds.), Paleozoic sequence stratigraphy, biostratigraphy and biogeography: studies in honor of J. Granville ("Jess") Johnson. Geol. Soc. Am. Spec. Pap., vol. 321, pp. 113–129.

Klapper, G., Becker, R.T., 1999. Comparison of Frasnian (Upper Devonian) conodont zonations. Boll. Soc. Paleontol. Ital. 37, 339–348.

Klapper, G., Feist, R., Becker, R.T., House, M.R., 1993. Definition of the Frasnian/Famennian stage boundary. Episodes 16, 433–441.

Klemme, H.D., Ulmishek, G.F., 1991. Effective petroleum source rocks of the world: stratigraphic distribution and controlling depositional factors. AAPG Bull. 75, 1809–1851.

Levasseur, S., Birck, J., Allègre, C., 1998. Direct measurement of femtomoles of osmium and the $^{187}Os/^{186}Os$ ratio in seawater. Science 282, 272–274.

Louvat, P., Allègre, C.J., 1997. Present denudation rates on the island of Reunion determined by river geochemistry: basalt weathering and mass budget between chemical and mechanical erosions. Geochim. Cosmochim. Acta 61, 3645–3669.

Ludwig, K.R., 1980. Calculation of uncertainties of U–Pb isotope data. Earth Planet. Sci. Lett. 46, 212–220.

Ludwig, K., 2003. Isoplot Version 3: a Geochronological Toolkit for Microsoft Excel. Geochronology Center Berkeley, Berkeley.

Marshall, J.E.A., Hemsley, A.R., 2003. A Mid Devonian seed-megaspore from East Greenland and the origin of the seed plants. Palaeontology 46, 647–670.

Martin, C.E., Peucker-Ehrenbrink, B., Brunskill, G.J., Szymczak, R., 2000. Sources and sinks of unradiogenic osmium runoff from Papua New Guinea. Earth Planet. Sci. Lett. 183, 261–274.

Martin, C.E., Peucker-Ehrenbrink, B., Brunskill, G., Szymczak, R., 2001. Osmium isotope geochemistry of a tropical estuary. Geochim. Cosmochim. Acta 65, 3193–3200.

McCutcheon, S.R., Anderson, H.E., Robinson, P.T., 1997. Stratigraphy and eruptive history of the Late Devonian Mount Pleasant Caldera Complex, Canadian Appalachians. Geol. Mag. 134, 17–36.

McGhee Jr., G.R., 1996. The Late Devonian Mass Extinction: the Frasnian/Famennian Crisis. Columbia University Press, New York.

McGregor, D.C., McCutcheon, S.R., 1988. Implications of spore evidence for Late Devonian age of the Piskahegan Group, southwestern New Brunswick. Can. J. Earth Sci. 25, 1349–1364.

McLaren, D.J., 1970. Time, life and boundaries. J. Paleontol. 44, 801–815.

Meyer-Berthaud, B., Scheckler, S.E., Wendt, J., 1999. *Archaeopteris* is the earliest known modern tree. Nature 398, 700–701.

Mosbrugger, V., 1990. The Tree Habit in Land Plants. Springer, Berlin.

Murphy, A.E., Sageman, B.B., Hollander, D.J., 2000. Eutrophication by decoupling of the marine biogeochemical cycles of C, N, and P: a mechanism for the Late Devonian mass extinction. Geology 28, 427–430.

Nier, A.O., 1937. The isotopic constitution of osmium. Phys. Rev. 52, 885.

Over, D.J., 1997. Conodont biostratigraphy of the Java Formation (Upper Devonian) and the Frasnian–Famennian boundary in western New York State. In: Klapper, G., Murphy, M.A., Talent, J.A. (Eds.), Paleozoic sequence stratigraphy, biostratigraphy and biogeography: studies in honor of J. Granville ("Jess") Johnson. Geol. Soc. Am. Spec. Pap., vol. 321, pp. 161–177.

Over, D.J., 2002. The Frasnian/Famennian boundary in central and eastern United States. Palaeogeogr. Palaeoclimatol. Palaeoecol. 181, 153–169.

Oxburgh, R., 1998. Variations in the osmium isotope composition of sea water over the past 200,000 years. Earth Planet. Sci. Lett. 159, 183–191.

Pegram, W.J., Turekian, K.K., 1999. The osmium isotopic composition change of Cenozoic sea water as inferred from a deep-sea core corrected for meteoritic contributions. Geochim. Cosmochim. Acta 63, 4053–4058.

Peucker-Ehrenbrink, B., Hannigan, R.E., 2000. Effects of black shale weathering on the mobility of rhenium and platinum group elements. Geology 28, 475–478.

Peucker-Ehrenbrink, B., Ravizza, G., 2000. The marine osmium isotope record. Terra Nova 12, 205–219.

Ravizza, G., Esser, B.K., 1993. A possible link between the seawater osmium isotope record and weathering of ancient sedimentary organic matter. Chem. Geol. 107, 255–258.

Ravizza, G., Peucker-Ehrenbrink, B., 2003. Chemostratigraphic evidence of Deccan volcanism from the marine osmium isotope record. Science 302, 1392–1395.

Ravizza, G., Turekian, K.K., 1989. Application of the $^{187}Re–^{187}Os$ system to black shale geochronometry. Geochim. Cosmochim. Acta 53, 3257–3262.

Ravizza, G., Turekian, K.K., 1992. The osmium isotopic composition of organic-rich marine sediments. Earth Planet. Sci. Lett. 110, 1–6.

Ravizza, G., Turekian, K.K., Hay, B.J., 1991. The geochemistry of rhenium and osmium in recent sediments from the Black Sea. Geochim. Cosmochim. Acta 55, 3741–3752.

Ravizza, G., Norris, R.N., Blusztajn, J., Aubry, M.P., 2001. An osmium isotope excursion associated with the late Paleocene thermal maximum: evidence of intensified chemical weathering. Paleoceanography 16, 155–163.

Retallack, G.J., 1997. Early forest soils and their role in Devonian global change. Science 276, 583–585.

Richards, B.C., Ross, G.M., Utting, J., 2002. U–Pb geochronology, lithology and biostratigraphy of tuff in the upper Famennian to Tournaisian Exshaw Formation: evidence for a mid-Paleozoic magmatic arc on the northwestern margin of North America. Can. Soc. Petrol. Geol. Mem. 19, 158–207.

Rotondo, K.A., Over, D.J., 2000. Biostratigraphic age of the Belpre Ash (Frasnian), Chattanooga and Rhinestreet shales in the Appalachian Basin. Geol. Soc. Am. Abstr. Program., vol. 32, p. A70.

Sageman, B.B., Murphy, A.E., Werne, J.P., Ver Straeten, C.A., Hollander, D.J., Lyons, T.W., 2003. A tale of shales: the relative roles of production, decomposition, and dilution in the accumulation of organic-rich strata, Middle–Upper Devonian, Appalachian basin. Chem. Geol. 195, 229–273.

Savoy, L.E., Harris, A.G., Mountjoy, E.W., 1999. Extension of lithofacies and conodont biofacies models of Late Devonian to Early Carboniferous carbonate ramp and black shale systems, Southern Canadian Rocky Mountains. Can. J. Earth Sci. 36, 1281–1298.

Scheckler, S.E., 1986. Geology, floristics and paleoecology of Late Devonian coal swamps from Appalachian Laurentia. Ann. Soc. Geol. Belg. 109, 209–222.

Scheckler, S.E., 2003. Consequences of rapid expansion of Late Devonian forests. Geol. Soc. Am. Abstr. Program., vol. 35, p. 385.

Schindler, E., 1990. Die Kellwasser-Krise (hohe Frasne-Stufe, Ober-Devon). Gött. Arb. Geol. Paläontol. 46, 115.

Selby, D., Creaser, R.A., 2003. Re–Os geochronology of organic-rich sediments: an evaluation of organic matter analysis. Chem. Geol. 200, 225–240.

Selby, D., Creaser, R.A., 2005. Direct radiometric dating of the Devonian–Mississippian time-scale boundary using the Re–Os black shale geochronometer. Geology 33, 545–548.

Selby, D., Creaser, R.A., Stein, H.J., Markey, R.J., Hannah, J.L., 2007. Assessment of the ^{187}Re decay constant by cross calibration of Re–Os molybdenite and U–Pb zircon chronometers in magmatic ore systems. Geochim. Cosmochim. Acta 71, 1999–2013.

Singh, S.K., Trivedi, J.R., Krishnaswami, S., 1999. Re–Os isotope systematics in black shales from the Lesser Himalaya: their chronology and role in the ^{187}Os/^{188}Os evolution of seawater. Geochim. Cosmochim. Acta 63, 2381–2392.

Smoliar, M.I., Walker, R.J., Morgan, J.W., 1996. Re–Os isotope ages of Group IIA, IIIA, IVA, and IVB iron meteorites. Science 271, 1099–1102.

Stearn, C.W., 1987. Effect of the Frasnian–Famennian extinction event on the stromatoporoids. Geology 15, 677–679.

Steemans, P., Fang, X., Streel, M., 1996. Retizonomonoletes hunanensis Fang et al. 1993 and the Lepidophyta morphon. Mem. Inst. Geol. Univ. Louvain 36, 73–88.

Streel, M., 2000. The late Famennian and early Frasnian datings given by Tucker et al. are biostratigraphically poorly constrained. Subcom. Dev. Strat. Newsletter 17, 59.

Streel, M., Loboziak, S., 1996. Middle and Upper Devonian miospores. In: Jansonius, J., McGregor, D.C. (Eds.), Palynology: Principles and Applications. Am. Assoc. Strat. Palynol. Found. Contrib. Series, vol. 2, pp. 575–587.

Taylor, A.S., Lasaga, A.C., 1999. The role of basalt weathering in the Sr isotope budget of the oceans. Chem. Geol. 161, 199–214.

Thompson, J.B., Newton, C.R., 1988. Late Devonian mass extinction. Episodic climatic cooling or warming? In: McMillan, N.J., Embry, A.F., Glass, D.J. (Eds.), Devonian of the world. Can. Soc. Petrol. Geol. Mem., vol. 14, pp. 29–34.

Trapp, E., Kaufmann, B., Mezger, K., Korn, D., Weyer, D., 2004. Numerical calibration of the Devonian–Carboniferous boundary: two new U- Pb isotope dilution -thermal ionization mass spectrometry single-zircon ages from Hasselbachtal (Sauerland, Germany). Geology 32, 857–860.

Tucker, R.D., Bradley, D.C., Ver Straeten, C.A., Harris, A.G., Ebert, J.R., McCutcheon, S.R., 1998. New U–Pb zircon ages and the duration and division of Devonian time. Earth Planet. Sci. Lett. 158, 175–186.

Völkening, J., Walczyk, T., Heumann, K.G., 1991. Osmium isotope ratio determinations by negative thermal ionization mass spectrometry. Int. J. Mass Spectrom. Ion Process. 105, 147–159.

Weary, D.J., Ryder, R.T., Nyahay, R., 2000. Thermal maturity patterns (CAI and %R_o) in the Ordovician and Devonian rocks of the Appalachian Basin in New York State. USGS Open File Rep. 00-0496.

Woodhouse, O.B., Ravizza, G., Kenison-Falkner, K., Statham, P.J., Peucker-Ehrenbrink, B., 1999. Osmium in seawater: vertical profiles of concentration and isotopic composition in the eastern Pacific Ocean. Earth Planet. Sci. Lett. 173, 223–233.

Ziegler, W., Sandberg, C.A., 1990. The Late Devonian standard conodont zonation. CFS, Cour. Forsch.inst. Senckenb. 121, 115.